Performance analysis of an all-optical half-subtracter based on XGM in SOA at 20 Gbps

KARAMDEEP SINGH[a,*], GURMEET KAUR[b], MANINDER LAL SINGH[a]
Department of Electronics Technology, Guru Nanak Dev University, Amritsar, Punjab, 143005, India
Department of Electronics & Communication Engineering, Punjabi University, Patiala, Punjab, 147002, India

Implementation of all-optical algebraic and arithmetic operations is fundamental for successful realization of complex all-optical signal processing (AOSP) tasks. Over the past few years, a number of All-optical computing devices such as half-adder, full-adder etc. have evolved based on 2nd ($\chi^{(2)}$) order and 3rd ($\chi^{(3)}$) order non-linear effects. In this paper, design and performance analysis of an all-optical half-subtracter based on cross-gain modulation (XGM) in bulk type semiconductor optical amplifier (SOA) capable of operating at 20 Gbps have been performed. A co-propagating structure has been utilized for the design purposes, which nullifies requirement of additional assisting light sources. Extinction ratios (ER) and quality factors (Q-Factor) of order of greater than 9.389 dB and 7.29, respectively have been achieved for half-subtracter outputs. Performance analysis has been performed by varying order and width (τ_{FWHM}) of input gaussian data pulse trains. Gaussian return-to-zero (RZ) data pulses of 3rd order and width (τ_{FWHM}) = 0.5 have been identified as optimum input pulses.

(Received February 16, 2016; accepted April 6, 2017)

Keywords: Cross-gain modulation (XGM), Semiconductor optical amplifier (SOA), All-optical signal processing (AOSP), All-optical logic gates

1. Introduction

In the past few years, due to tremendous advances in semiconductor-based technologies, all-optical signal processing (AOSP) solutions have emerged, which have the potential to replace the existing electronic signal processing (ESP) implementations in high capacity networks as key enabling technology [1]. As ESP is marred by incapability to process large amount of data at ultra-high speed due to formation of bottlenecks created during rapid optical-electronic-optical (O-E-O) conversions, as signal processing is carried out in electronic domain. AOSP can overcome O-E-O - limitation, as it is possible to directly process the data in optical domain itself, utilizing photonic logic devices for switching purposes [2, 3]. In present day scenarios, AOSP is being considered as viable option to replace ESP as key enabling technology in routers and other switching devices utilized in high capacity wavelength division multiplexing (WDM) networks [4]. For the realization of complex and application specific AOSP tasks, basic logic gates serve as building blocks [1, 5]. Further, an enormous amount of research activity is being witnessed in past decade in the field of design of all-optical arithmetic devices such as half-adder, half-subtracter and full-adder etc. using variety of non-linear effects in 2nd ($\chi^{(2)}$) & 3rd ($\chi^{(3)}$) order non-linear mediums such as periodically poled lithium niobate (PPLN) [6, 7] and semiconductor optical amplifiers (SOA) [8-15] thus paving the way for idea of realization of All-optical computer in near future, having ultra-high processing speed and minimum electronic intervention. SOA based schemes are superior as compared to other approaches due to their small size and lesser power requirement [16].

Several researchers have introduced a number of approaches over the years. The first ever approach was based on ultrafast nonlinear interferometer (UNI) utilizing SOA [1]. Tsiokos et al. (2004) [1] reported an UNI based all-optical half-adder capable of operating up to 10 Gbps. But proposed UNI based designs was bulky and polarization sensitive.

The second approach reported was utilization of non-linear effects in structure consisting of SOA followed with an optical bandpass filter. Kim et al. (2006) [5] proposed an all-optical half-adder based on above said scheme exhibiting 6.1 dB ER (dB) at 10 Gbps. Lei et al. (2012) [13] implemented a full-subtracter and full-adder based on similar approach consisting of 4 parallel SOAs achieving ERs > 8 dB at 40 Gbps bit rate. Dai et al. (2013) [15] also used this approach to realize all-optical half-adder and half-subtracter at 10 Gbps exhibiting 14 dB ER. This approach was simpler as compared to other schemes and only limitation of this approach was requirement of very good output optical bandpass filter.

Another popular approach was exploitation of 2nd ($\chi^{(2)}$) order non-linear effects such as cascaded sum frequency generation and difference frequency generation (cSFG-DFG) in PPLN waveguides [6, 7]. Wang et al. (2007) [6] implemented all-optical half-adder using cSFG-DFG in PPLN waveguide which can operate up to 40 Gbps. Shen et al. (2011) [7] proposed an all-optical full-adder utilizing 5 cascaded PPLNs. The PPLN based approaches are Integrable, stable, but marred by slow carrier dynamics of PPLN waveguides.

In another technique reported, cross-phase modulation (XPM) in SOA was used inside mach-zehnder interferometer (MZI) to implement arithmetic circuits [2, 8, 11]. Cherri and Al-Zayed (2010) [8] implemented all-optical modified signed-digit adders, Ghosh et al. 2011b [11] designed an all-optical half-adder using above said methodology. Gayen et al. (2012) [2] described a similar approach, utilizing quantum-dot semiconductor optical amplifiers (QD-SOAs) instead of using bulk SOAs in MZI structure to implement all-optical half-adder at 160 Gbps. The only limitation was that 4 QD-SOAs were required for the successful implementation of this scheme.

The last reported scheme was based on asymmetrically placed SOA in sagnac arrangement, which is also known as terahertz optical asymmetric demultiplexer (TOAD) arrangement [14]. Gayen et al. (2012) [14] proposed an all-optical carry lookahead adder (CLA) based on TOAD Sagnac arrangement demonstrating contrast ratio (CR) of 38.30 dB. However, TOAD based devices are faster but bulkier as compared to other approaches.

In this paper, an all-optical half-subtracter demonstration based on XGM has been done at 20 Gbps operating bit rate without use of assist light sources using gaussian pulses. Particularly, the proposed half-subtracter is an improved version of that presented in Ref. [15], from the perspective of operating bit rate, which is 20 Gbps in the present case. Further, optimum input gaussian pulse shape has been identified by analyzing the proposed half-subtracter performance in terms of Q-Factor and ER (dB) by presenting it with gaussian pulses of various orders and duty cycles.

The article is organized as follows: In section 1, the concept of AOSP has been introduced along with its underlying mechanics in brief; particular emphasis has been given to all-optical arithmetic logic circuit design and previous work in this area. The concept of half-subtracter along with underlying non-linear phenomena used for the implementation i.e. XGM has been presented in Section 2. Section 3, describes system setup and device parameters of SOAs and other components used in design of proposed half-subtracter. Results and discussions are presented in Section 4. Section 5, concludes this paper.

2. Concept and operational principle

A half-subtracter subtracts two one bit numbers (A & B) and generates two output bits, difference and borrow. The truth table of half-subtracter is illustrated in Table 1, below [6, 15]:

Table 1. Truth table of half-subtracter [6, 15].

Input Signal		Half-Subtracter Outputs		
A	B	Borrow A-B	Borrow B-A	Difference
0	0	0	0	0
0	1	1	0	1
1	0	0	1	1
1	1	0	0	0
Logic Functions		$\overline{\boldsymbol{A}}.\boldsymbol{B}$	$\boldsymbol{A}.\overline{\boldsymbol{B}}$	A ⊕ B XOR

From Table 1, it can be noted that difference output of half-subtracter can be represented by XOR function, whereas Borrow can be represented by $A.\overline{B}$ or $\overline{A}.B$, depending on whether A is subtrahend or minuend and vice-versa [6, 15]. Therefore, three logic functions i.e. XOR, $A.\overline{B}$ and $\overline{A}.B$ are required, in order to successfully implement the half-subtracter circuit. However, XOR function can be realized by simply ORing $A.\overline{B}$ and $\overline{A}.B$ signals i.e. $A \oplus B = \overline{A}.B + A.\overline{B}$.

In order to realize $A.\overline{B}$ and $\overline{A}.B$ functions in optical domain, XGM phenomena, has been utilized in present communication. XGM is a non-linear phenomena usually observed in SOA, in which gain of signal centered at one wavelength can be affected by signal at other wavelength due to carrier density changes taking place in SOA. The gain coefficient g (t, z) of SOA is given as [17]:

$$g(t,z) = [N(t,z) - N_t]a\Gamma L \tag{1}$$

where $N(t,z)$ is carrier density, N_t is transparency carrier density, a is differential gain constant, Γ is confinement factor and L in length of amplifier. Basically, in travelling wave SOA's, having facet reflectivity < 10^{-4}, when an optical signal passes through gain medium, the excited electrons present in gain medium starts settling to ground state giving almost all energy to passing signal i.e. amplification of optical signal takes place. However, amplification process consumes a large number of carriers, thus gain is reduced to lower levels for a small interval, which is termed as gain saturation [5]. The generalized formula of gain variation in SOA due to XGM caused crosstalk is given by [5, 15-16, 18-20]:

$$\Delta g(t_1, z_1) = \frac{a\Gamma}{\tau P_L}\left[\frac{I\tau}{wqt_a}\exp\left(\frac{\Delta P_1}{\tau}\right) + \sum_{n=1}^{M}\frac{(-1)^n}{P_L^{n-1}}Lexp\left(\frac{\Delta P_n}{\tau}\right)\right]$$

$$\times [\overline{N}(t_n, z_n) - (N(t,z) - N_t)\overline{P}^{n-1}(t_{n-1}, z_{n-1})] \tag{2}$$

where Δg is small gain variation, t is time, I is injection current, z is position along propagation direction, t_a is thickness of active region, τ is carrier recombination time, M is total number of channels, $P_i(t,z)$ is the power in ith channel, w is width of SOA active region, t_{eff} is effective

thickness of SOA active region, $\Gamma = \frac{t_a}{t_{eff}}$ is the confinement factor, $P_L = \frac{\partial P(t_1,z_1)}{\partial t_1}$ is derivative power coefficient and derivative carrier density is $\overline{N} = \frac{\partial N(t_1,z_1)}{\partial t_1}$. It can be observed from equation number (2), that gain of one channel is affected by gain variation of other channels present simultaneously inside SOA active region, as given by 2nd term in equation number (2) i.e. $\sum_{n=1}^{M} \frac{(-1)^n}{P_L^{n-1}} Lexp\left(\frac{\Delta P_n}{\tau}\right)$. This so called gain saturation phenomena can be used to realize logic functions utilizing pump-probe configuration as illustrated in Fig. 1 [5, 15-16, 18-21].

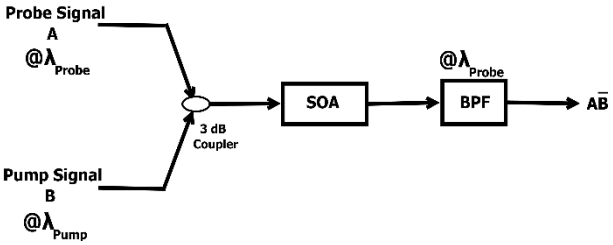

Fig. 1. Pump-probe technique [15].

As depicted in Fig. 1, inside an SOA, a signal having high energy (i.e. pump signal B) and one having lesser energy (i.e. probe signal A) are combined. If pump signal is present i.e. B = 1, then due to amplification of high energy pump signal, the carriers in SOA gain medium are depleted causing gain saturation phenomena, further causing suppression of probe pulses due to absence of carriers. However, if high energy pump signal is absent i.e. B = 0, then, probe signal gets amplified and survives suppression. A band pass filter (BPF) centered at probe wavelength (λ_{probe}) is used to extract the resulted $A.\overline{B}$ signal. Similarly, $\overline{A}.B$ function can be generated using the similar configuration with this time, roles of pump and probe reversed, i.e. signal A as high energy pump signal and signal B as low energy probe signal [5, 15-16, 18-20].

3. System setup

The system setup utilized for the demonstration of XGM based all-optical half-subtracter is shown in Fig. 2. Two mode locked laser diodes (MLLDs), centered at ~1547 nm and ~1550 nm having 0 dBm and 20 dBm peak powers, respectively have been used as carrier sources. A variable optical attenuator (VOA) has been used to optimize the power of carrier signal before feeding it to mach-zehnder modulator (MZM). Two pseudo random binary sequence (PRBS) generators having 2^7-1 long sequence length are used to generate data patterns at 20 Gbps which are further converted into RZ gaussian electric pulses using RZ gaussian drivers before insertion into MZM. Modulated signals from both branches (A & B) are then split into further two branches using 3 dB splitters.

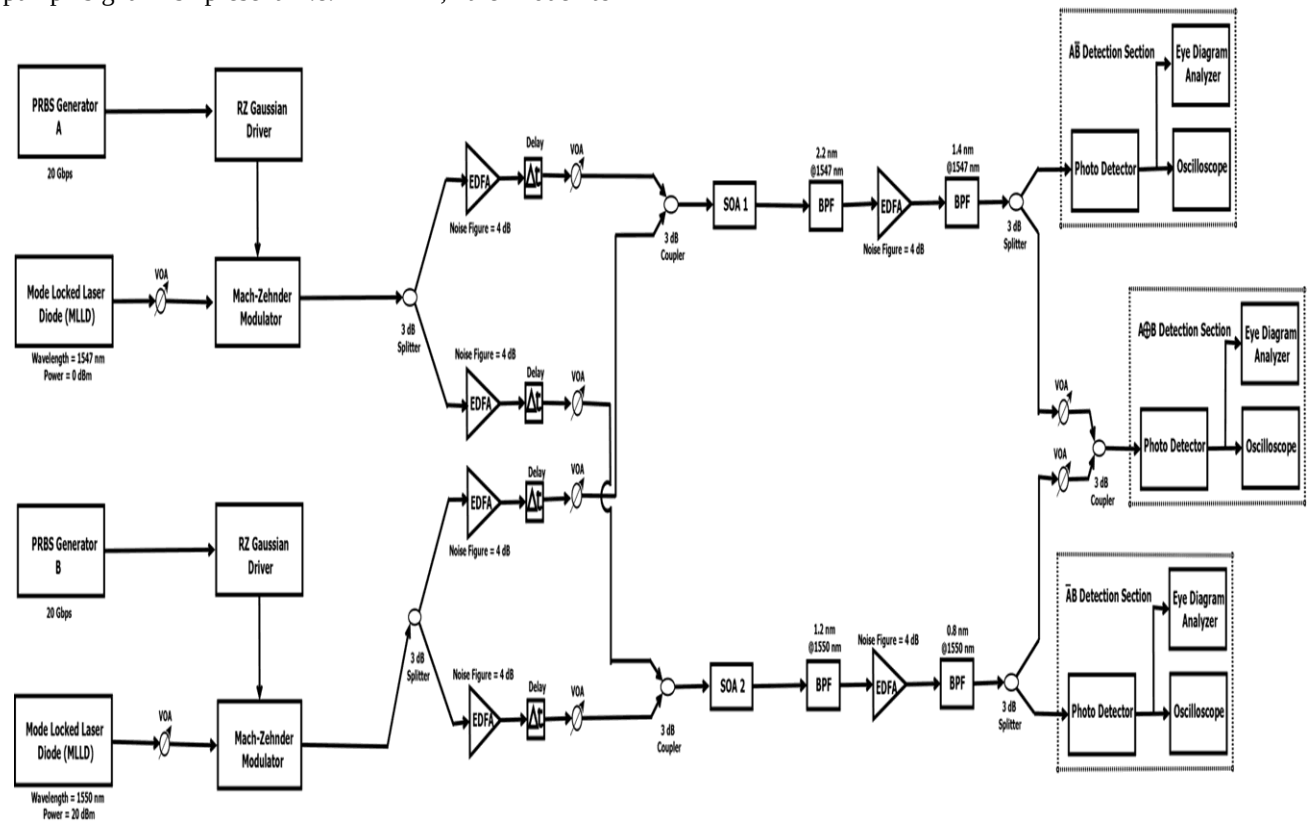

Fig. 2. System setup of half-subtracter based on XGM in SOA

Now two out of the four branches carry signal A, whereas other two carry signal B. One signal each from branches carrying opposite signals (A & B) are coupled into SOA 1 & SOA 2 after optimizing power levels and time difference alignment using a combination of erabium doped fiber amplifier (EDFA), VOA and delay line. All the EDFA's utilized in the experiment have 4 dB noise figure (NF). The average power levels of signal A & B before insertion into SOA 1 are -9.57 dBm & 5.407 dBm, respectively, as A acts as probe and B as pump in this case. Similarly, signals A and B are power optimized to -3.130 dB and -6.193 dB, respectively, before coupling to SOA 2, as in this case signal A serves as pump, whereas signal B as probe. The input and output power spectra of signals before and after SOA1 and SOA 2 are illustrated in Fig. 3. (a-b) below:

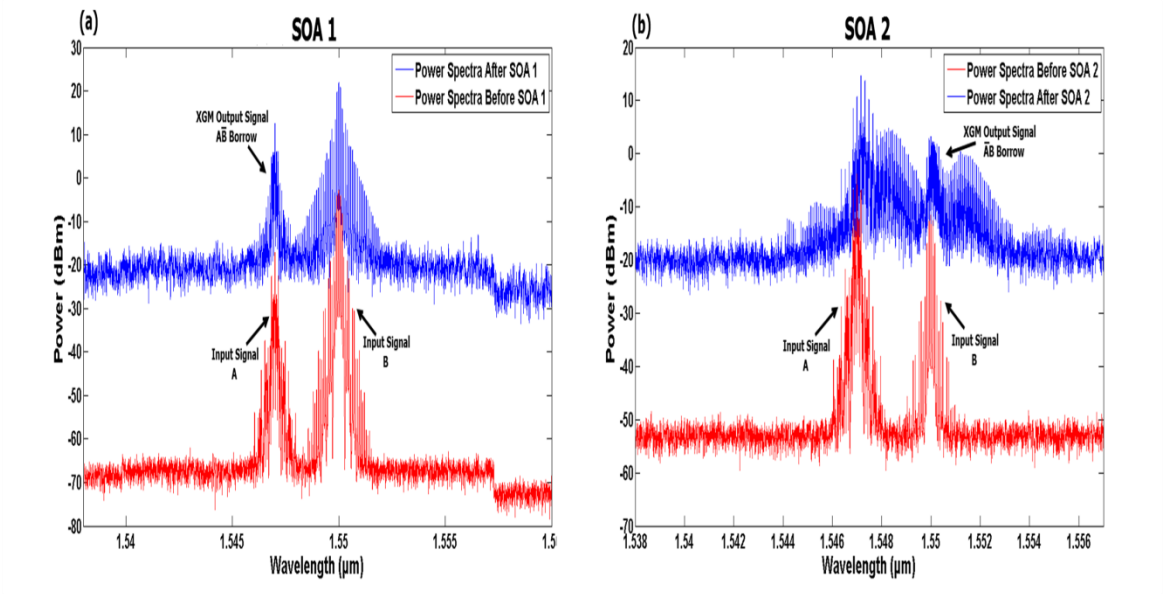

Fig. 3. (a) Power spectra calculated before and after SOA 1, (b) Power spectra calculated before and after SOA 2

As it can be observed from Fig. 3 (a) that signal $A.\overline{B}$ i.e. borrow signal is generated by XGM process between signal A as pump signal and signal B as probe signal inside SOA 1. Using two stages of band pass filtering centered at 1547 nm, $A.\overline{B}$ signal is extracted and fed to detection section as illustrated in Fig. 2. Similarly, $A.\overline{B}$ signal is produced by XGM phenomena inside SOA 2, with roles of Signals A and B reversed. $\overline{A}.B$, borrow signal is extracted by two stage BPFs centered at 1550 nm. The extracted $A.\overline{B}$ and $\overline{A}.B$ signals are then fed into their respective detection sections. Power spectra of each signal are widened due to chirp after passing through respective SOA. Each detection section comprising of combination of low pass filter (LPF) and PIN photo detector having 10 Gain, 1 A/W Responsivity with 10 nA dark current converts the optical signal to electric domain. The detected signal is then fed to eye diagram analyzer and oscilloscope for further analysis. In order to generate XOR signal, the BPF filtered versions of $A.\overline{B}$ and $\overline{A}.B$ signals are combined with a 3 dB coupler, after optimizing signal power with VOA and aligning time differences between each other using delay lines. The proposed scheme is based on XGM in SOA. In order to enhance the XGM process in SOA, optimized SOAs have been used in present scheme. Injection currents (I) of SOA 1 and SOA 2 are 660 mA and 410 mA, respectively. Optimized parameter values of SOAs used are listed in Table 2:

Table 2. XGM optimized SOA 1 and SOA 2 parameters

Sr. No.	*Name of Parameter*	*SOA 1*	*SOA 2*
1.	Amplifier length (L)	600 μm	500 μm
2.	Active layer width (w)	6.5 μm	2.67 μm
3.	Active layer thickness (t)	0.08 μm	0.117 μm
4.	Optical confinement factor (Γ)	0.4	0.35
5.	Loss	0 m^{-1}	0 m^{-1}
6.	Differential gain (a)	2.78×10^{-20} m^2	2.78×10^{-20} m^2
7.	Transparency carrier density (N_t)	1.4×10^{24} m^3	1.4×10^{24} m^3
8.	Linewidth enhancement factor (α)	0.1	5
9.	Linear recombination coefficient (A)	1.43×10^{8} s^{-1}	1.43×10^{8} s^{-1}
10.	Bimolecular recombination coefficient (B)	1×10^{-16} m^3/s	1×10^{-16} m^3/s
11.	Auger recombination coefficient (C)	3×10^{-41} m^6/s	3×10^{-41} m^6/s
12.	Initial carrier density (N)	3×10^{24} m^{-3}	2×10^{24} m^{-3}

4. Results and discussions

In order to assess the performance of XGM based all-optical half-subtracter, variety of input data patterns were presented at 20 Gbps bit rate. For example, data patterns A (11110010) and B (10101010) were chosen to demonstrate the operation of All-Optical half-subtracter graphically as depicted in Fig. 4. (a-e):

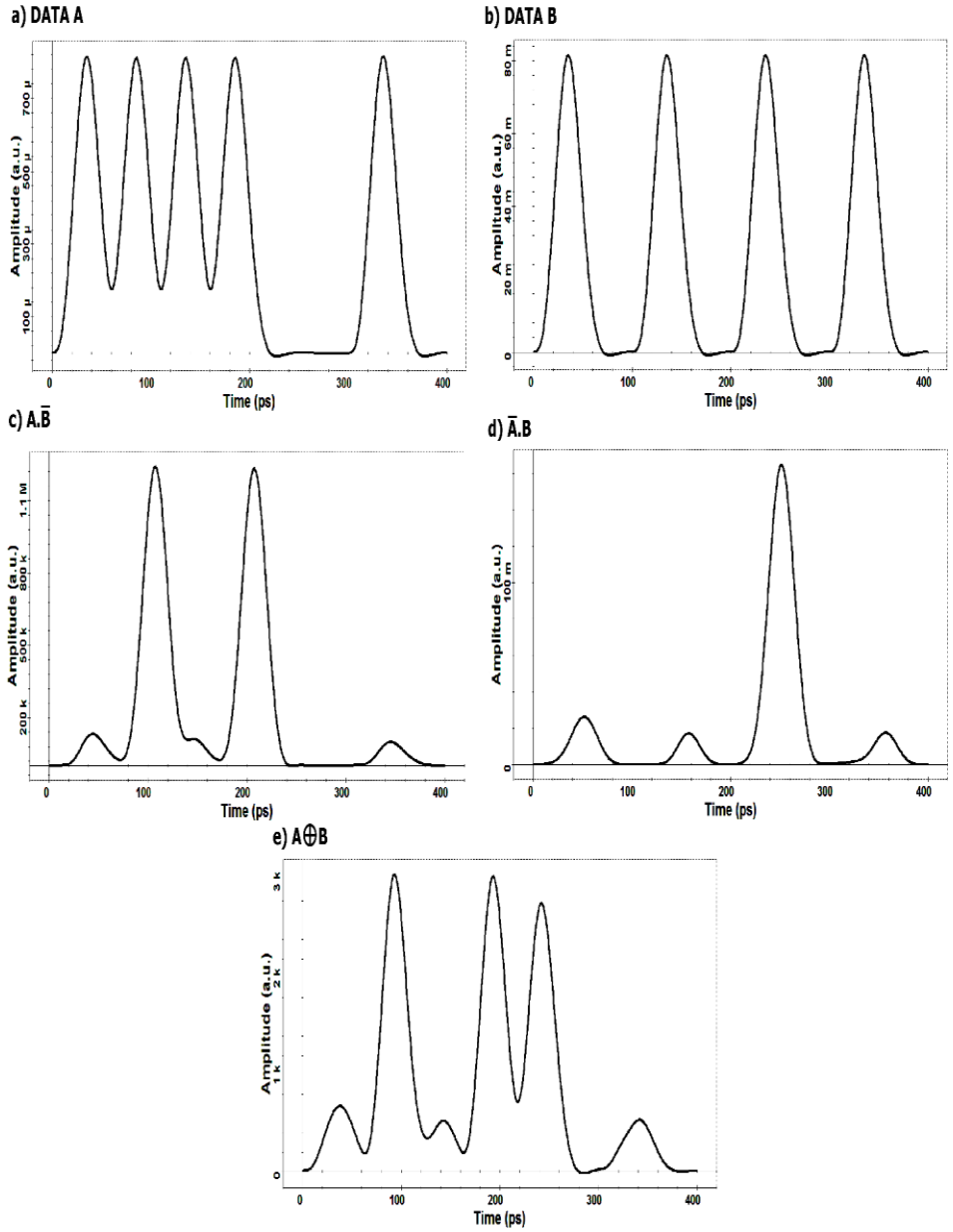

Fig. 4. (a-b) Waveforms of input signals A & B, (c-e) Waveforms of output signals $A.\overline{B}$, $\overline{A}.B$ & $A \oplus B$.

Fig. 4 (a-b) & (c-e) shows the input and output data traces of half-subtracter at 20 Gbps bit rate, respectively. It can be seen that correct output sequence for borrow outputs i.e. $A.\overline{B}$ (01010000), $\overline{A}.B$ (00001000) & difference output $A \oplus B$ (01011000) have been obtained, which verifies the correct operation of the proposed scheme. However, due to timing mismatch between input pump and probe signals, there are some discrepancies in output signals pulse shapes and pulse widths. Further, some data patterning effect is also observed in half-subtracter Fig. 4 (c-e) outputs to some extent, which can be avoided by using SOAs having short gain recovery dynamics. Fig. 5 (a-c) reports the eye diagrams of output signals considering 1024 bits long simulated sequence having 64 samples/ bit.

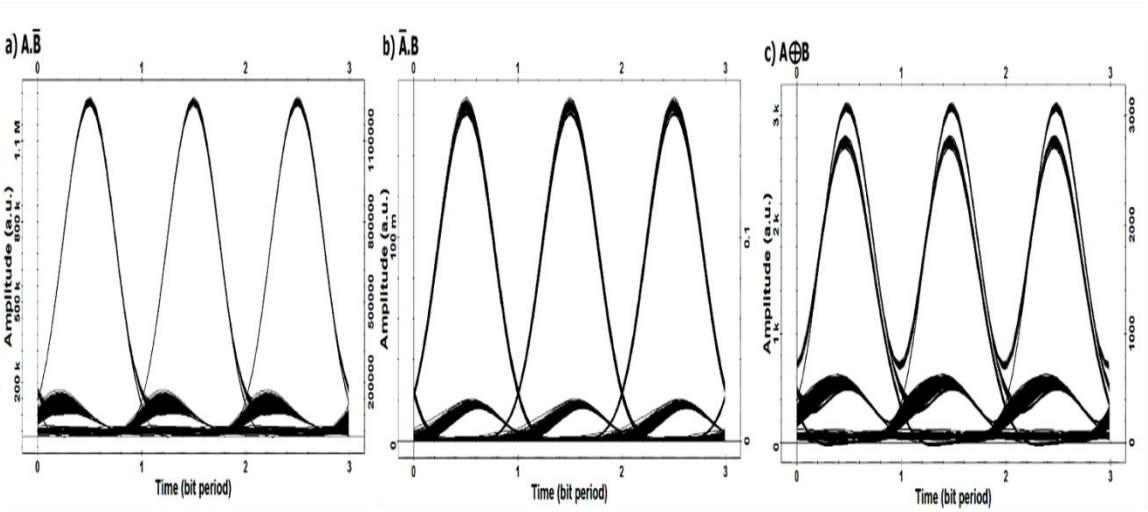

Fig. 5. (a-c) Eye diagrams of output signals $A.\overline{B}$, $\overline{A}.B$ & $A \oplus B$

It can be observed from Fig. 5 (a-c), that clear and open diagrams have been obtained for each output of half-subtracter indicating error free operation of proposed approach. Two performance metrics: Q-Factor & ER (dB) have been used to evaluate the performance of proposed approach. The Q-Factor is given by following relation [2, 22, 23, 24]:

$$Q = \frac{P^1 - P^0}{\sigma^1 + \sigma^0} \tag{3}$$

where, P^1 & P^0 are average output power of high state (1-state) and low state (0-state), respectively. σ^1 and σ^0 are standard deviations of high state (1-state) and low state (0-state), respectively [2, 14, 22, 23, 24]. The second performance metric is ER which is defined as [2, 23, 25, 26]:

$$ER(dB) = 10log_{10}\left(\frac{P^1_{Min}}{P^0_{Max}}\right) \tag{4}$$

where P^1_{Min} and P^0_{Max} are minimum and maximum values of peak power of high state (1-state) and low state (0-state), respectively [2, 25, 26]. The Q-Factor and ER of the circuit should be high enough so that the high state (1-state) can distinguished from low-state (0-state). Maximum Q-factors of 48.25, 20.79 and 7.29 have been attained for $A.\overline{B}$, $\overline{A}.B$ and $A \oplus B$, respectively. Additionally, ER (dB) of 16.647 dB, 15.68 dB and 9.389 dB have been achieved for $A.\overline{B}$, $\overline{A}.B$ and $A \oplus B$, respectively. The results attained here reports improvement over results presented in Ref. [15] in terms of Q-Factor, ER (dB) at an improved operating bit rate as well. Further, research can be carried out to improve the performance of the proposed approach in terms of operating bit rate, using SOAs having lesser gain recovery time.

Further, performance analysis has been carried out to formulate optimum order and pulse width of gaussian pulse for achieving best possible performance of the half-subtracter in terms of Q-factor and ER (dB). The power profile of 20 Gbps optical gaussian pulse generated by both MZM's in Fig. 2 is given by equation number (5) [27]:

$$P_{A,B}(t) = \sum_{n=-\infty}^{+\infty} a_{nA,B} \frac{2\sqrt{ln2}P_0}{\sqrt{\pi}\tau_{FWHM}} exp\left(-\frac{4ln2(t-nT)^2}{\tau^2_{FWHM}}\right) \tag{5}$$

where is $P_{A,B}(t)$ output optical power, $a_{nA,B}$ is bit value (0 or 1) depending on input bit sequence, P_0 is energy in a single pulse and τ_{FWHM} is width of pulse [23]. In this analysis optimized parameters values of SOA 1 and SOA 2 used are presented in Table 2. These gaussian pulses have been used as pump and probe pulses in the half-subtracter. For analysis purpose, the order and width (τ_{FWHM}) of Gaussian pulse is varied between 0 to 5 and 0 to 1, respectively, and deviations in Q-Factor and ER (dB) are graphically presented below, for each output of half-subtracter i.e. borrow ($A.\overline{B}$, $\overline{A}.B$) and difference ($A \oplus B$) in Fig. 6 (a-f):

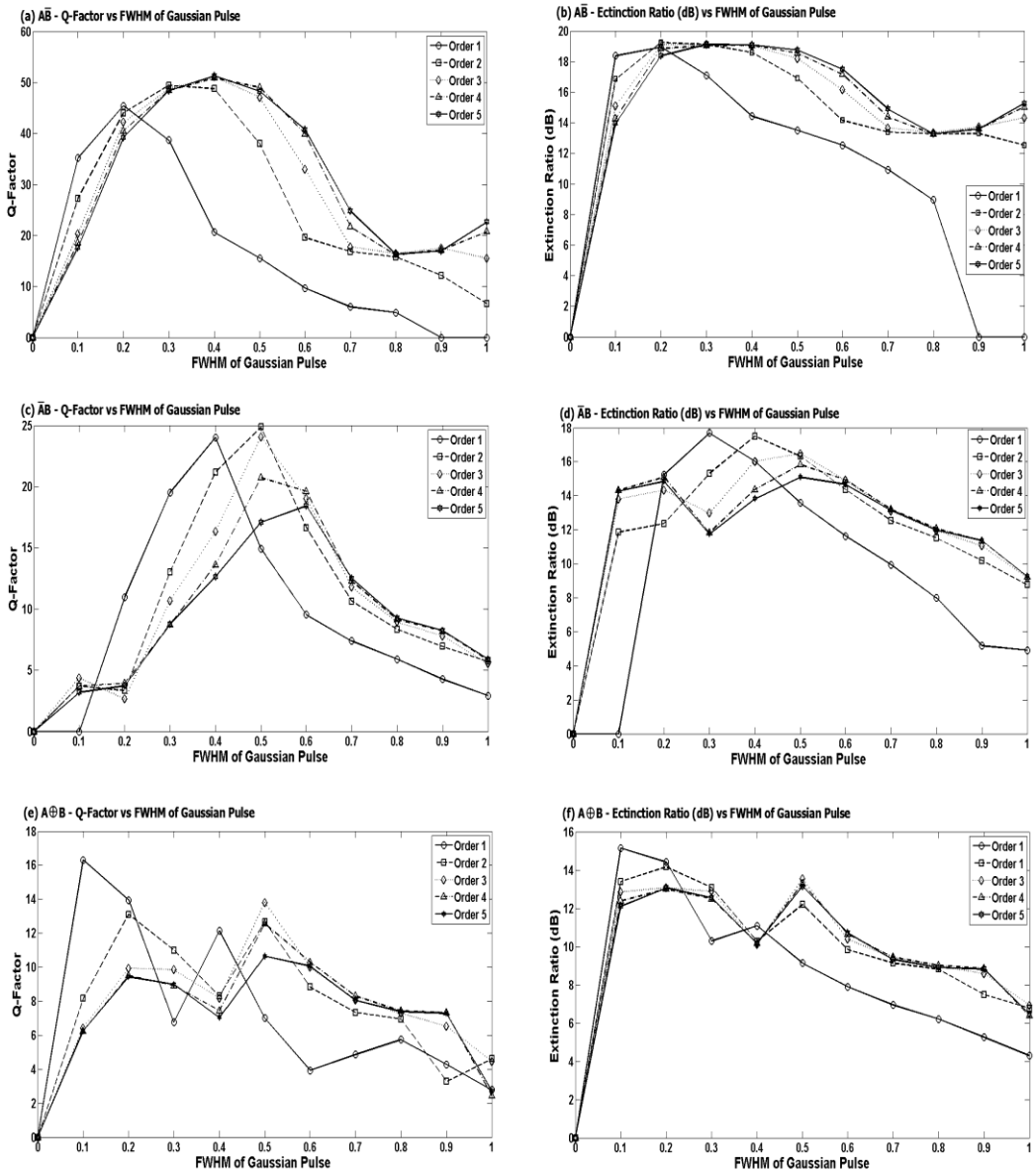

Fig. 6. (a), (c), (e) Variations of Q-Factor vs. FWHM (τ_{FWHM}) of Gaussian pulse for output signals $A.\overline{B}$, $\overline{A}.B$ (borrow) & $A \oplus B$ (difference) , respectively. (b), (d), (f) Variations of ER (dB) vs. FWHM (τ_{FWHM}) of Gaussian pulse for output signals $A.\overline{B}$, $\overline{A}.B$ (borrow) & $A \oplus B$ (difference), respectively

It can be observed from the Fig. 6 (a, c, e), by studying variations of Q-factor vs. FWHM (τ_{FWHM}) of gaussian pulse for each output of half-subtracter, i.e. borrow ($A.\overline{B}$, $\overline{A}.B$) and difference ($A \oplus B$) that best Q-Factor is achieved, when order of gaussian pulse is 3 and width is 0.5. The Q-factor vs. FWHM (τ_{FWHM}) of gaussian pulse variations for borrow ($A.\overline{B}$, $\overline{A}.B$) outputs exhibit an increasing trend for every order, when pulse width is varied from 0 to 0.5, but after this a diminishing trend has been observed as pulse width is increased from 0.5 to 1 in 0.1 wide steps, which may be attributed to the fact that energy carried by each pulse is enhanced due to increase in pulse width, but saturation power of two SOA's used is kept at a constant level during normal operation. So in case, when pulse width > 0.5, saturation process occurs early in SOAs then expected, which affects XGM between pump and probe signals, resulting in degradation in Q-factor of operation. Similar trends are reported while analyzing ER (dB) vs. FWHM (τ_{FWHM}) of gaussian pulse for each output of half-subtracter, i.e. borrow ($A.\overline{B}$, $\overline{A}.B$) and difference ($A \oplus B$) as shown in Fig. 6 (b, d, f). Maximum ER (dB) is attained when order and FWHM (τ_{FWHM}) of Gaussian pulse is 3 and 0.5, respectively for every output of half-subtracter. The Maximum Q-factor & ER (dB) values obtained for each output of half-subtracter borrow ($A\overline{B}$, $\overline{A}B$) and difference ($A \oplus B$) using Gaussian pulses of order 3 and τ_{FWHM} = 0.5 are summarized in Table 3, below:

Table 3. Q-factor and ER (dB) values for optimum input gaussian pulses having order = 3 and width = 0.5

Sr. No.	Output of half-subtracter	Q-Factor	Extinction Ratio (dB)
1.	Borrow ($A\bar{B}$)	48.25	16.647 dB
2.	Borrow ($\bar{A}B$)	20.79	15.68 dB
3.	Difference ($A \oplus B$)	7.29	9.389 dB

5. Conclusions

In this work, all-optical half-subtracter demonstration and performance analysis has been performed utilizing the gain non-linearity characteristics of semiconductor optical amplifier (SOA) at 20 Gbps without the use of extra assisting lights in a co-propagating configuration. In order to verify the proposed system various data patterns have been presented and clear and open eye diagrams have been obtained indicating error free operation. Further, optimum order and width of gaussian pulses used as input data signal has been defined by performing simulative analysis, in order to obtain acceptable ER (dB) and Q-Factor. ER (dB) of 16.647 dB, 15.68 dB and 9.389 dB have been achieved for half-subtracter outputs such as Borrow ($A.\overline{B}$, $\overline{A}.B$) and Difference ($A \oplus B$), respectively utilizing optimum Gaussian pulses of order 3 and width (τ_{FWHM}) = 0.5.

References

[1] D. Tsiokos, E. Kehayas, T. Vyrsokinos, T. Houbavlis, L. Stampoulidis, G. T. Kanellos, N. Pleros, G. Guekos, H. Avramopoulos, IEEE Photon. Technol. Lett. **16**(1), 284 (2004).

[2] D. K. Gayen, A. Bhattachryya, T. Chattopadhyay, J, N. Roy, J. Lightwave Technol. **30**(21), 3387 (2012).

[3] K. Singh, G. Kaur, Opt. Laser Technol. **69**, 122 (2015).

[4] R. Vilar, J. M. Martinez, F. Ramos, J. Marti, Opt. Express **16**(24), 19734 (2008).

[5] S. H. Kim, J. H. Kim, C. W. Choi, C. W. Son, Y. T. Byun, Y. M. Jhon, S. Lee, D. H. Woo, S. H. Kim, Opt. Express **14**(22), 10693 (2006).

[6] J. Wang, J. Sun, Q. Sun, Opt. Express **15**(4), 1690 (2007).

[7] J. Shen, S. Yu, P. Liao, Z. Chen, W. Gu, IEEE J Quantum Electron. **47**(9), 1195 (2011).

[8] A. K. Cherri, A. S. Al-Zayed, Optik – International Journal for Light and Electron Optics **121**(17), 1577 (2010).

[9] S. K. Garai, S. Mukhopadhyay, Optik – International Journal for Light and Electron Optics **121**(20), 1859 (2010).

[10] P. Ghosh, D. Kumbhakar, A. K. Mukherjee, K. Mukherjee, Optik – International Journal for Light and Electron Optics **122**(19), 1757 (2011).

[11] B. Ghosh, R. R. Pal, S. Mukhopadhyay, Optik – International Journal for Light and Electron Optics **122**(20), 1804 (2011).

[12] K. Mukherjee, Optik – International Journal for Light and Electron Optics **122**(13), 1188 (2011).

[13] L. Lei, J. Dong, Y. Zhang, H. He, Y. Yu, X. Zhang, Electron. Lett. **48**(7), 399 (2012).

[14] D. K. Gayen, J. N. Roy, R. K. Pal, Optik – International Journal for Light and Electron Optics **123**(21), 40 (2012).

[15] B. Dai, S. Shimizu, X. Wang, N. Wada, IEEE Photon. Technol. Lett. **25**(1), 91 (2013).

[16] A. Sharaiha, J. Topomondzo, M. Pascal, Opt. Commun. **265**(1), 322 (2006).

[17] G. P. Agrawal, N. A. Olsson, IEEE J. Quantum Electron. **25**(11), 2297 (1989).

[18] S. Kumar, A. E. Willner, Opt. Express **14**(12), 5092 (2006).

[19] M. Cabezón, A. Villafranca, J. J. Martinez, D. Izequierdo, I. Garcés, J. Lightwave Technol. **31**(8), 1178 (2013).

[20] Lovkesh, S. S. Gill, Optik – International Journal for Light and Electron Optics **122**(11), 978 (2011).

[21] S. Singh, Lovkesh, IEEE J. Sel. Top. Quantum Electron. **18**(2), 970 (2012).

[22] G. Kaur, M. L. Singh, M. S. Patterh, J. Opt. Fiber Commun. Res. **6**(1-6), 1 (2009).

[23] K. Singh, G. Kaur, M. L. Singh, Opt. Engg. **55**(7), 077104 (2016).

[24] K. Singh, G. Kaur, M. L. Singh, Photon. Netw. Commun. doi:10.1007/s11107-016-0677-5 (In press), (2016).

[25] K. Singh, G. Kaur, M. L. Singh, Opt. Fiber Technol. **24**, 56 (2015).

[26] K. Singh, G. Kaur, M. L. Singh, Opt. Quantum Electron. **48**(9), 418 (2016).

[27] H. Sun, Q. Wang, H. Dong, Z. Chen, N. K. Dutta, J. Jaques, A. B. Piccirilli, IEEE J. Quantum Electron. **42**(8), 747 (2006).

*Corresponding author: karamdeep1989@gmail.com